

ACCURATE LATENCY CHARACTERIZATION FOR VERY LARGE ASYNCHRONOUS SPIKING NEURAL NETWORKS

Mario Salerno, Gianluca Susi and Alessandro Cristini
Institute of Electronics, Rome University at Tor Vergata, Rome, Italy

Keywords: Neuron, Spiking Neural Network (SNN), Latency, Event-driven, Plasticity, Threshold, Neuromorphic, Neuronal group selection.

Abstract: The simulation problem of very large fully asynchronous Spiking Neural Networks is considered in this paper. To this purpose, a preliminary accurate analysis of the latency time is made, applying classical modelling methods to single neurons. The latency characterization is then used to propose a simplified model, able to simulate large neural networks. On this basis, networks, with up to 100,000 neurons for more than 100,000 spikes, can be simulated in a quite short time with a simple MATLAB program. Plasticity algorithms are also applied to emulate interesting global effects as the Neuronal Group Selection.

1 INTRODUCTION

A significant class of simulated neuromorphic systems is represented by *Spiking Neural Networks* (SNN), in which the neural activity consists of spiking events generated by firing neurons (E. M. Izhikevich, J. A. Gally, G. M. Edelman, 2004), (W. Maas, 1997). In order to consider realistic models, the simulation of the inner dynamics of the neurons can be very complex and time consuming (E. M. Izhikevich, 2004). Indeed, accurate neuron models consist of complex systems of non-linear differential equations, so that any actual simulation is computationally convenient only in the case of quite small networks. On the other hand, only in the case of large networks, a number of interesting global effects can be investigated, as the well known *Neuronal Group Selection*, introduced by Edelman (G. M. Edelman, 1987). In order to consider the simulation of large networks, it is important to introduce simplified models, in which any single neuron be able to produce a class of firing patterns quite similar to those of the biological counterpart. In this paper, a proper SNN model will be introduced, based on some fundamental properties of neurons. The proposed model is able to simulate large neuromorphic maps, up to 100,000 neurons.

A basic problem to realize realistic SNN concerns the apparently random times of arrival of the synaptic signals (G.L. Gernstein, B. Mandelbrot,

1964). Many methods have been proposed in the technical literature in order to properly desynchronizing the spike sequences; some of these consider transit delay times along axons or synapses (E. M. Izhikevich, 2006), (S. Boudkkazi, E. Carlier, N. Ankri, O. Caillard, P. Giraud, L. Fronzaroli-Molinieres and D. Debanne, 2007). A different approach introduces the *spike latency* as a neuron property depending on the inner dynamics (E. M. Izhikevich, 2007). Thus, the firing effect is not instantaneous, as it occurs after a proper delay time which is different in various cases. In this work, we will suppose this kind of desynchronization as the most effective for SNN simulation.

Spike latency appears as intrinsic continuous time delay. Therefore, very little sampling times should be used to carry out accurate simulations. However, as sampling times grow down, simulation processes become more time consuming, and only short spike sequences can be emulated. The use of the event-driven approach can overcome this difficulty (D'Haene, B. Schrauwen, J. V. Campenhout and D. Stroobandt, 2009), since continuous time delays can be used and the simulation can easily proceed to large sequence of spikes. Indeed, simulations of more than 100,000 spikes are possible by this method in a quite short computing time.

In the proposed model, classical learning algorithms can easily be applied in order to get proper adjustment of the synaptic weights. In such a

way, adaptive neural networks can be implemented in which proper plasticity rules are active. In presence of input signals, the simulation of the whole network shows the selection of neural groups in which the activity appears very high, while it remains at a quite low level in the regions among different groups. This auto-confinement property of the network activity seems to remain stable, even when the considered input is terminated.

The paper is organized as follows: description and simulation of some basic properties of the neuron, such as threshold and latency; introduction of the simplified model on the basis of the previous analysis, description of the network structure, plasticity algorithm, input structure, simulation results and performance tests.

2 LATENCY CHARACTERIZATION

Different kinds of neurons can be considered in nature, with special and peculiar properties (S. Ramon y Cajal, 1909-1911). On the other hand, many models have been introduced and compared in terms of biological plausibility and computational cost. Antipodes are the *Integrated and Fire* (L. Lapique, 1907) and the *Hodgkin-Huxley Model* (A.L. Hodgkin, A.F. Huxley, 1952), the first one characterized by low computational cost and low fidelity, while the second is a quite complete representation of the real case.

In the latter case, the model consists of four differential equations describing membrane potential, activation of Na⁺ and K⁺ currents, and inactivation of Na⁺ current (E. M. Izhikevich, 2007). From an electrochemical point of view, the neuron can be characterized by its *membrane potential* V_m .

In the simulation starting case, the neuron lies in its resting state, i.e. $V_m = V_{rest}$ (*Resting Potential*), until an external excitation is received.

The membrane potential varies by integrating the input excitations. Since contributions from outside are constantly added inside the neuron, a significant accumulation of excitations may lead the neuron to cross a threshold, called *firing threshold* TF (E. M. Izhikevich, 2007), so that an output spike can be generated.

However, the output spike is not immediately produced, but after a proper delay time called *latency* (R. FitzHugh, 1955). Thus, the latency is the delay time between exceeding the membrane potential threshold and the actual spike generation.

From a physiological point of view, such a delay time is usually attributed to the slow charging of the dendritic tree, as well as to the action of the A-current, namely the voltage-gated transient K⁺ current with fast activation and slow inactivation. The current activates quickly in response to a depolarization and prevents the neuron from immediate firing. With time, however, the A-current inactivates and eventually allows firing (E. M. Izhikevich, 2007). This phenomenon is affected by the amplitudes and widths of the input stimuli and thus rich dynamics of latency can be observed, making it very interesting for the global network desynchronization.

It is quite evident that latency concept strictly depends on an exact definition of the threshold level. However, strictly speaking, the true threshold is not a fixed value, as it depends on the previous activities of the neuron, as shown by the Hodgkin-Huxley equations (A.L. Hodgkin, A.F. Huxley, 1952). Indeed, a neuron is similar to a dynamical system, in which any actual state depends on the previous ones.

The first work addressing the threshold from a mathematical point of view was *FitzHugh* (R. FitzHugh, 1955), who defined the *Quasi Threshold Phenomenon* (*QTP*). A finite maximum latency is defined, but neither a true discontinuity in response nor an exact threshold level are considered. Indeed, with reference to the squid giant axon model, it has been pointed out that the membrane fluctuations for experimental observations or insufficient accuracy for the simulators, make not possible to establish an exact value of the threshold. To this purpose, in figures 1a and 1b, it is shown that the neuron behaviour is very sensitive with respect to small variations of the excitation current.

Nevertheless, in the present work, an appreciable maximum value of latency will be used. This value is determined by simulation and applied to establish a reference threshold point. When the membrane potential becomes greater than the threshold, the latency appears as a function of V_m . To this purpose, proper simulations have been carried out for single neurons.

3 SINGLE NEURON SIMULATIONS

Significant latency properties will be analysed in this section. To this purpose, the NEURON Simulation Environment (<http://www.neuron.yale.edu/neuron/>) has been used, a tool for quick development of

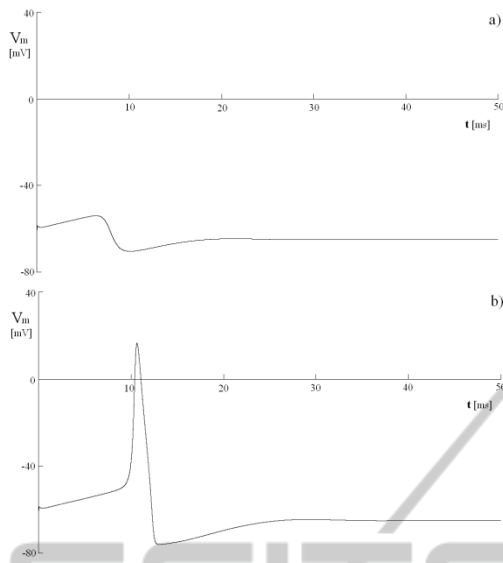


Figure 1: Change of membrane potential, caused by two current pulses of 0.01 ms applied to the initial resting state at $t = 0$. The amplitudes are 0.64523 nA (fig. 1a) and 0.64524 nA (fig. 1b). The behaviours, obtained by the simulator NEURON, appear very sensitive with respect to the current amplitude and justify the name “All-Or-None law”, adopted in neuroscience in these cases.

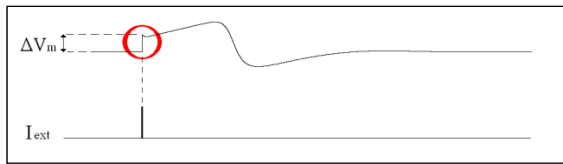


Figure 2: Instantaneous variation of ΔV_m for an impulsive current injected I_{ext} .

realistic models for single neurons, on the basis of Hodgkin-Huxley equations.

In the field over the threshold level, the latency can directly be related to input current pulses, received as stimuli from spikes generated by afferent neurons. Since the instantaneous variations of membrane potential (ΔV_m) appear almost linear with respect to the related current pulses, the latency can also be represented as a function of the membrane potential. Note that, starting from the resting state ($V_{rest} = -65\text{ mV}$), an excitatory pulse of 1 nA (0.01 ms time width) corresponds to $\Delta V_m = 10\text{ mV}$.

Three significant cases have been simulated, using the integration step of 0.00125 ms and the current pulse width of 0.01 ms .

α) Case of Single Excitatory Current Pulses

Starting from the resting state, an input current pulse of proper amplitude, able to cause output spike after

a proper latency time, has been applied. Simulating a set of examples, with current pulses in the range $[0.64524 \div 10]\text{ nA}$, the latency as a function of the pulse amplitude, or else of the membrane potential V_m , has been determined. The latency behaviour is shown in Fig. 3, in which it appears decreasing, with an almost hyperbolic shape. The threshold level corresponds to the pulse amplitude equal to 0.64524 nA , with the maximum latency of 10.6313 ms . Pulses with less amplitudes are under the threshold level, so that no output spikes are more obtained in these cases.

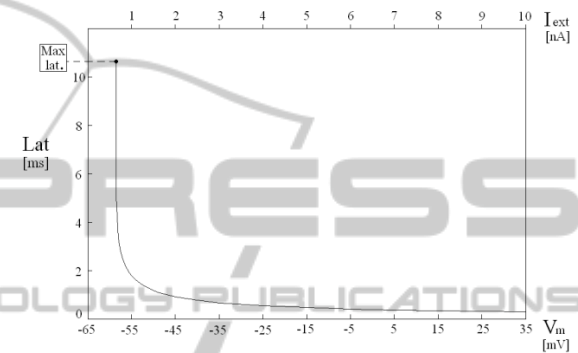


Figure 3: Latency as a function of the membrane potential (or else of the current amplitude I_{ext} , equivalently).

β) Case of Two Excitatory Current Pulses

Starting from the resting state, after a first input current pulse, able to cause an output spike, a second pulse has been applied in the latency interval, in order to analyse the corresponding latency speed up in the firing process. As the first pulse is of fixed amplitude (equal to 0.64524 nA), the overall latency is a function of the second pulse amplitude (varying in the range $[0.001 \div 5]\text{ nA}$) and of the time interval Δ , between the two excitatory current pulses.

In fig. 4, the behaviours of the overall latency time, i.e. the time between the first pulse and the output spike, in function of the second pulse amplitude, are shown, for different values of Δ . Note that the overall latency always decreases with the second pulse amplitude. However, while the effect of the second pulse is quite relevant for low values of Δ , it becomes almost irrelevant when Δ is high, i.e. almost equal to the value of the latency corresponding to the first pulse only.

γ) Case of a First Excitatory and a Second Inhibitory Current Pulse.

Starting from the resting state, after a first input current pulse, able to cause an output spike, a second pulse has been applied in the latency interval, after the time interval Δ . The second pulse is negative, so

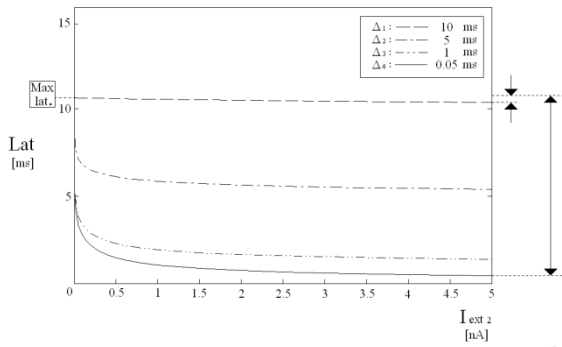


Figure 4: Set of behaviours corresponding to excitatory-excitatory stimuli. Each curve represents the overall latency in function of the second stimulus amplitude, for a fixed time interval Δ between the two stimuli. The effect is greater in the case of low values of Δ .

that an inhibitory effect is produced. As the first pulse is of fixed amplitude (equal to 3.0 nA , which ensures that the membrane potential is carried quite over the threshold), the second one is of varying amplitude (from -0.01 nA , until it be still possible to appreciate the output spike).

Once the second pulse is applied, the main effect is the generation of an action potential delay increment, caused by the inhibitor pulse. The more the inhibitor pulse is strong, the greater the delay resulted in the generation of action potential. In addition, more the inhibitor pulse is timely, greater is the latency produced. Even in this case, the overall latency is a function of the second pulse amplitude (fig.5). It is worth to emphasize that, as the interval between the two pulses becomes relatively large, the influence of the inhibitor is cancelled.

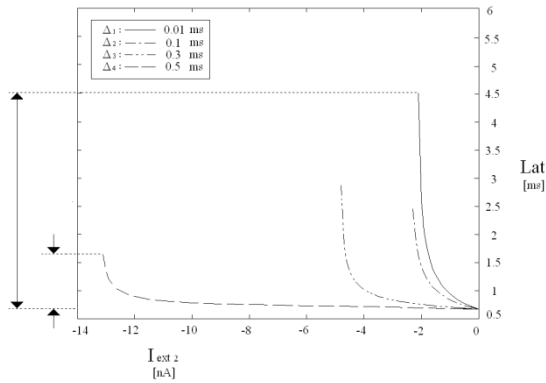


Figure 5: Set of behaviours corresponding to excitatory-inhibitory stimulation. Each curve represents the latency in function of the inhibitory stimulus amplitude, for a fixed time interval Δ between the two stimuli. The latency variation is greater in the case of low values of Δ .

4 SIMPLIFIED NEURON MODEL IN VIEW OF LARGE NEURAL NETWORKS

In the simplified model, a number of normalized and simplified quantities are introduced, to represent their physical counterpart. The membrane potential is represented by a normalized real positive number \mathcal{S} , said the inner state of the neuron, defining the value $\mathcal{S} = 0$ as the resting state. The firing threshold corresponds to the value \mathcal{S}_0 , so that the activity of the neuron can properly be classified, as *passive mode* if $\mathcal{S} < \mathcal{S}_0$, and *active mode* if $\mathcal{S} > \mathcal{S}_0$.

In *active mode*, the neuron is ready to fire, and the latency is modelled by a real positive quantity t_f , called *time-to-fire*. To this purpose, a bijective correspondence between the state \mathcal{S} and t_f is introduced, called the *firing equation*. A simple choice for the normalized *firing equation* is the following one:

$$t_f = 1 / (\mathcal{S} - 1), \text{ for } \mathcal{S} > \mathcal{S}_0 \quad (1)$$

In the model, t_f is a measure of the latency, as it represents the time interval in which the neuron remains in the active state. Thus, *time-to-fire* decreases with time and, as it gets to zero, the *firing event* occurs. If the normalized firing threshold \mathcal{S}_0 is chosen such that

$$\mathcal{S}_0 = 1 + \varepsilon \quad (2)$$

the maximum value of *time-to-fire* is equal to

$$t_{f,max} = 1 / \varepsilon \quad (3)$$

Equation (1) is a simplified model of the behaviour shown in section 3, fig. 3. Indeed, as the latency is a function of the membrane potential, *time-to-fire* is dependent from the state \mathcal{S} , with a similar shape, like a rectangular hyperbola. The simulated and the denormalized *firing equation* behaviours are compared in fig. 6.

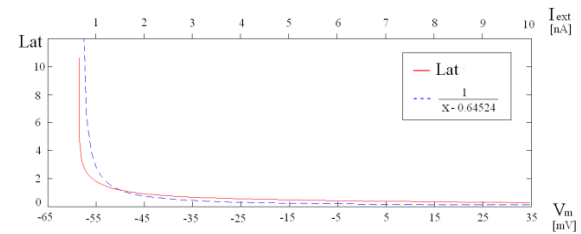


Figure 6: Comparison between the latency behaviour and that of the denormalized firing equation. The two behaviours present a shape similar to a rectangular hyperbola.

In a similar way, it could easily be proved that also the behaviours shown in fig.s 4 and 5 can correctly be modelled by the proper use of the *firing equation*. Indeed, it is important to stress that equation (1) must be applied as a bijective relation. Thus, in the case of more input pulses, the following steps must be considered.

a) As the appropriate first input is applied, the neuron enters in active mode, with a proper state S_A and a corresponding time-to-fire t_{fA} .

b) According to the bijective *firing equation*, as time goes on, t_{fA} decreases to the value $t_{fB} = t_{fA} - \Delta$ and the corresponding inner state S_A increases to the new value S_B , until the second input is received.

c) After the interval Δ , the second input is received. It is clear that now the new state S_B is to be considered. The state S_B is now affected by the input and, the greater is Δ (in the interval $0 < \Delta < t_{fA}$), the greater the corresponding value of S_B . Thus, the effect of the second input pulse becomes irrelevant for great values of Δ .

This peculiar property proves the good validity of the proposed model.

In the model, the *firing event* consists in the generation of the output signal. When the *firing event* occurs in a certain neuron, it is said a *firing neuron*. The *firing event* consists of the following steps.

A) Transmission of the firing signals through the output synapses connected to the receiving neurons, said *burning neurons*. In the proposed model, the transmission is considered instantaneous, thus the transmitted signals are impulses of amplitude equal to the *presynaptic weight*, Pr .

B) Resetting the *inner state* S to the rest state $S = 0$.

C) For each directly connected burning neuron k , modification of its inner state S_k as

$$S_k = S_k + Pr Pw \tag{4}$$

in which Pw is the related *postsynaptic weight* of the considered synapse.

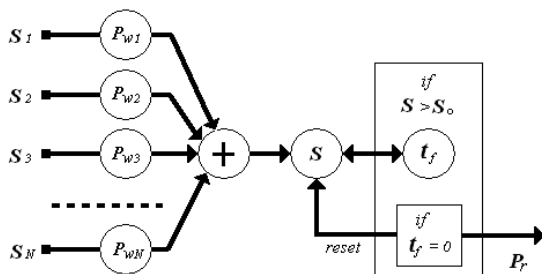


Figure 7: Proposed model for the neuron.

It is evident that the model introduces a modulated delay for each firing event. This delay strictly depends on the inner dynamics of the neuron.

Time-to-fire and *firing equation* are basic concepts to make asynchronous the whole neural network. Indeed, if the firing equation is not introduced, and time-to-fire is always equal to zero, the fire event would be produced exactly when the state S becomes greater than S_0 , and this would happen at the same time for all the neurons reaching their active modes. Thus, the behaviour of the whole network would be synchronous. The definition of time-to-fire as a continuous variable let the firing process dependent on the way by which each firing neuron has reached its active mode.

In the classical neuromorphic systems, neural networks are composed by excitatory and inhibitory neurons. In our model, the presynaptic weight Pr are chosen positive for excitatory and negative for inhibitory neurons.

5 NETWORK STRUCTURE

The connection map of the neurons is defined establishing for each firing neuron (in which the firing event is produced) the burning neurons directly connected to it by proper synapses, through proper postsynaptic weights. It is evident that the difference between firing and burning neurons is only considered to define the related synapses and the network topology. Indeed, any neuron can be minded either firing or burning, whether it generates or receives a spiking signal. The whole synapse distribution can be stored in a general $N \times N$ matrix $[P_w J]$, in which N is the total number of neurons. Each entry of this matrix represents the post-synaptic weight corresponding to a firing vs. a burning neuron. If such a synapse is not present, the entry is zero, and thus, as the synaptic connection net among neurons is usual quite not complete, the matrix $[P_w J]$ will be sparse. Moreover, for large number of neurons, the complete $N \times N$ matrix cannot easily be stored. Thus, proper sparse matrix technique has been applied in the simulation program, in order to optimise the memory requirements.

Many network topologies could be implemented by this technique. In the proposed simulation program, the simple case of local like connections is considered, as in the case of *Cellular Neural Networks* (L.O.Chua, L.Yang, 1988). Each firing neuron is directly connected to a number of burning neurons belonging to a proper neighbourhood. The

local connection maps are shown in fig.s 8 and 9, where grids of excitatory (*en*) and inhibitory (*in*) neurons are indicated. The following classes of synapse kinds are defined: s_{ee} , s_{ei} , s_{ie} , while synapses s_{ii} are never present (the subscript *e* stands for excitatory neuron, and *i* for inhibitory neuron).

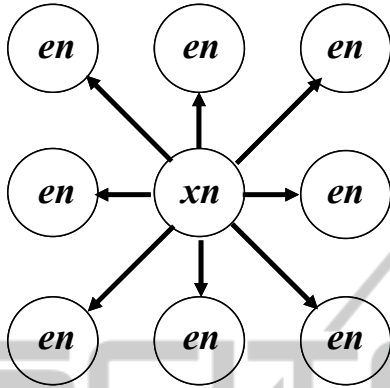


Figure 8: Map of synapses s_{ee} , and s_{ie} ; *xn* stands for excitatory or inhibitory firing neuron, while *en* for excitatory burning neurons.

As shown in the literature, greater neighbourhood is applied for inhibitory neurons (G. M. Edelman, 1987). Therefore, in the case of synapses s_{ei} , inhibitory burning neurons are not neighbouring to the related excitatory firing counterpart. Note that fig.s 8 and 9 refer to the case of minimum neighbourhood.

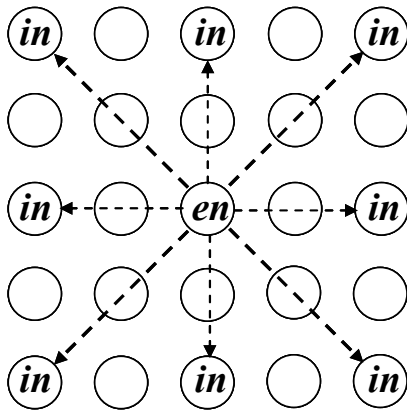


Figure 9: Map of synapses s_{ei} ; *en* stands for excitatory firing neuron, while *in* for inhibitory burning neurons.

6 PLASTICITY RULES

Plasticity consists in the proper variation of the postsynaptic weights P_w , according to the neuron dynamics. All the P_w weights are bounded from a

minimum to a maximum value, and are always positive quantities. The classical Hebb rule was proved not to be quite suitable to properly model the complex plasticity behaviour of natural nervous system. In this paper, three plasticity effects have been implemented, according to (G. M. Edelman, 1987).

Exponential decay: all postsynaptic weights are decreased to the minimum value in an exponential way with proper time constant.

Heterosynaptic enhancement: when a burning event occurs from a certain synapse, the postsynaptic weight is increased to the maximum value, in function of previous burnings on the same neuron, in a specified time window (heterosynaptic window) from other synapses.

Homosynaptic enhancement: when a burning event occurs from a certain synapse, the postsynaptic weight is increased to the maximum value, in function of previous burnings on the same neuron and from the same synapse, occurred in a specified time window (homosynaptic window).

The growing rates (increase, decrease) related to hetero and homosynaptic rules are properly chosen.

7 SIMULATION

The proposed neural paradigm has been implemented in a simple MATLAB program. The simulation method proceeds looking for the next firing event occurring in the whole network. It can be seen that the proposed model is not suitable for a classical simulation procedure based on a specified sampling time. Indeed, as small this sampling time is chosen, two contiguous firing events are likely to occur in the whole net, in a less time interval. Thus, larger networks are simulated, smaller time intervals can occur. Time continuity in the simulation is then necessary, in particular for very fast dynamics. On the other hand, the use of very little sampling times can make very slow the simulation process.

Then, it is evident that event-driven simulation method is quite suitable to the proposed neural model. To this purpose, a proper matrix is introduced in which all the active neurons are stored, together with their time-to-fire values. Looking for the lower time-to-fire, the next firing event is identified in term of the firing neuron and the instant of the event. Then, the active neuron matrix is properly updated and the new time value is identified in the event driven process. Therefore, the simulation proceeds in a very fast way.

Network activity is based upon two steps.

1. Searching for the active neuron with the minimum time-to-fire

2. Evaluation of the effects of the firing event to all the burning neurons.

A necessary condition to maintain the activity is that unless one neuron be active in every time. If this is not the case, all the neurons are passive and the activity is terminated.

Burning events can be classified in four classes.

a. *Passive Burning*. In this case a passive neuron remains still passive after the burning event, i.e. the inner state is always less than the threshold.

b. *Passive to Active Burning*. In this case, a passive neuron becomes active after the burning event, i.e. the inner state becomes greater than the threshold, and the proper value of the time-to-fire can be evaluated. This is possible only in the case of excitatory firing neurons. The case α), analysed in section 3, belongs to this class of burnings.

c. *Active Burning*. In this case an active neuron, affected by the burning event, still remains active, while the inner state can be increased or decreased and the time-to-fire is properly modified. The cases β) and γ), analysed in section 3, belong to this class of burnings.

d. *Active to Passive Burning*. In this case an active neuron comes back to the passive mode. This is only possible in the case of inhibitor firing neurons. The inner state decreases and becomes less than the threshold. The related time-to-fire is cancelled.

Since any firing event always makes passive the firing neuron, the frequency of burnings of classes a) and b) must be sufficiently high. Indeed, burnings of class c) only modify the time evolution, and burning of class d) reduces the global activity. On this basis, many criteria can be introduced to evaluate the activity level of the whole network.

A significant parameter by which the global stability can be controlled is the presynaptic weight P_r , which represents the firing signal amplitude for each firing neuron in the net. Indeed, lower values of P_r lead to the reduction of total number of firing neurons, up to the deadline of any activity. On the contrary, higher values of P_r let increase the firing number, up to the saturation of the system. A quite correct value of P_r can be chosen considering the number of synapses starting from a given firing neuron (fan-out, f_o). Since each firing event produces the resetting of inner state S from S_θ (normalized threshold) to θ , the value S_θ can be thought distributed among all the synapses outgoing the neuron. Thus, a useful choice is $P_r = S_\theta / f_o$. This

choice was proved quite likely to guarantee the network stability.

7.1 Input Structure

Input signals are considered quite similar to firing spikes, though depending from external events. Input firing sequences are connected to some specific neurons through proper external synapses. Thus, proper input burning neurons are chosen. External firing sequences are multiplied by proper postsynaptic weights in the burning process. Also these weights are affected by the described plasticity rules, thus the same inputs can be connected to different burning neurons, showing different effects in the various cases.

7.2 Simulation Tests

Several simulation tests have been carried out on the proposed neural paradigm. In many cases, random values for the postsynaptic weights have been chosen as starting point for the simulation.

If proper input sequences are simulated, and if the proposed plasticity rules are active, some properties of the network evolution have been verified, in particular the selection of specific neural groups, in which the activity appears in a quite high level, while it remains lower in the regions among different groups. This auto-confinement property of the network activity seems to remain stable, even if the considered input is terminated.

As an example, we propose a neural network of the following characteristics:

$$\begin{aligned} \text{Number of excitatory neurons} &= 18060 \\ \text{number of inhibitory neurons} &= 2021 \\ \text{number of external sources} &= 25 \end{aligned}$$

The excitatory neurons are located in a bidimensional grid. The size of the grid is 140×129 . Since a neighbourhood equal to 4 is chosen, a total number of 1,608,220 postsynaptic weights is implemented. As an initial choice, these weights have been assigned in a random way, from a minimum to a maximum value. In order to carry out a network able to show an initial activity, proper starting values for the states S have been assigned. In this way, the initial number of active neurons was equal to 2452.

In fig. 10, the map of the network is represented, in which every neuron is shown as a point. Clearer points represent neurons in the cases of lower values of their inner states S , while darker points refer to the cases of higher S .

We present here the simulation parameters of the network after a number of firings equal to 22518. The normalized *inner simulation time* is equal to 116.5, where the number of active neurons is reduced to 1096. The new neuron map is shown in fig. 11, in which the activity of the network appears not uniform, as that shown in fig. 10. Indeed, five specific groups are now present, in which the most of active neurons are grouped. The bounds of groups are quite sharp and the activity in the regions among them is near to zero.

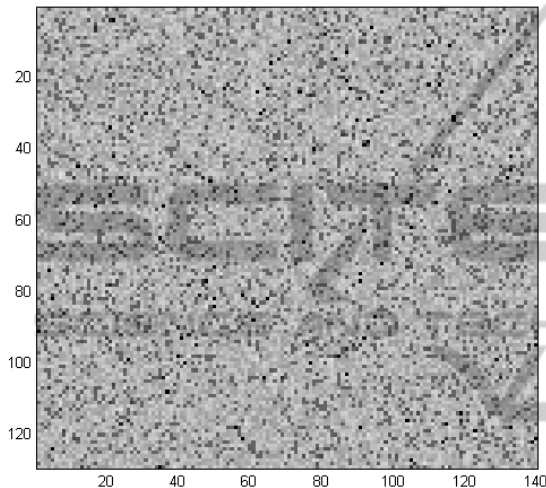


Figure 10: Map of the neural network used in the simulation test. Each point represents a single neuron. Brighter points stand for low values of S , darker for higher values. The map refers to the random initial configuration, before processing.

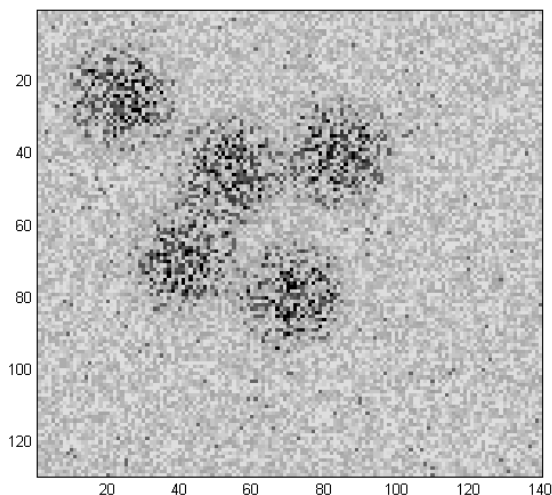


Figure 11: The same map of fig. 10, after simulation. The Neuronal Group Selection clearly appears.

The simulation parameters, involved in the process from the initial map of fig. 10 to that of fig. 11, are the following ones:

<i>Number of firing</i>	= 22,517
<i>Number of burnings:</i>	
<i>passive</i>	= 1,163,500
<i>passive-to-active</i>	= 21,020
<i>active</i>	= 568,891
<i>active-to-passive</i>	= 1223

The parameters involved in the plasticity rules are the following ones:

<i>Number of etherosynaptic upgrading</i>	= 39,469,900
<i>Number of homosynaptic upgrading</i>	= 2,341,430

Typical time performances of the simulation test is about 11 minutes, on a Pentium dual core 2.5 GHz (ram: 2GB).

8 CONCLUSIONS

Neural networks based on a very simple model have been introduced. The model belongs to the class of Spiking Neural Networks in which a proper procedure has been applied to accounting for latency times. This procedure has been validated by accurate latency analyses, applied to single neuron activity by simulation methods based on classical models. The firing activity, generated in the proposed network, appears fully asynchronous and the firing events consist of continuous time sequences. The simulation of the proposed network has been implemented by an event-driven method, allowing the possibility of simulating very large network by a quite simple MATLAB procedure. The simulation shows the appearance of the well known Neuronal Group Selection, when proper input sequences and proper plasticity rules are applied.

Future works in the field could be about the stability analysis of the firing activity and of the plasticity rules, in order to generate permanent functional groups in the whole network. The results related to the analysis of chaotic firing processes in single groups seem also very promising.

REFERENCES

- E. M. Izhikevich, J. A. Gally, G. M. Edelman, 2004: "Spike-timing dynamics of neuronal groups", 14:933–944. Oxford University press.

- W. Maas, 1997: “*Networks of Spiking Neurons: The Third Generation of Neural Network Models*”. Elsevier Science Ltd.
- E. M. Izhikevich, 2004: “*Which model to use for cortical spiking neurons?*” IEEE Transactions on neural networks, Vol. 15
- G. M. Edelman, 1987: “*Neural Darwinism: The Theory of Neuronal Group Selection*”. Basic Books, New York.
- G. L. Gernstein, B. Mandelbrot, 1964: “*Random walk models for the spike activity of a single neuron*”. Biophysical journal, Vol.4.
- E. M. Izhikevich, 2006: “*Polychronization: computation with spikes*”. Neural Computation 18, 18:245-282.
- S. Boudkkazi, E. Carlier, N. Ankri, O. Caillard, P. Giraud, L. Fronzaroli-Molinieres and D. Debanne, 2007: “*Release-Dependent Variations in Synaptic Latency: A Putative Code for Short- and Long-Term Synaptic Dynamics*”. *Neuron*, volume 56, issue 6.
- E. M. Izhikevich, 2007: “*Dynamical Systems in Neuroscience: The Geometry of Excitability and Bursting*”. The MIT press.
- M. D’Haene, B. Schrauwen, J. V. Campenhout and D. Stroobandt, 2009: “*Accelerating Event-Driven Simulation of Spiking Neurons with Multiple Synaptic Time Constants*”. Neural computation, apr. 21(4).
- S. Ramon y Cajal, 1909, 1911: “*Histologie du Systeme Nerveux de l’Homme et des Vertebres, vol. I & II*”.
- L. Lapicque, 1907: “*Recherches quantitatives sur l’excitation électrique des nerfs traitée comme une polarization*”.
- A. L. Hodgkin, A.F. Huxley, 1952: “*A quantitative description of membrane current and application to conduction and excitation in nerve*”, Journal of Physiology, 117, 500-544.
- R. FitzHugh, 1955: “*Mathematical models of threshold phenomena in the nerve membrane*”. Bull. Math.Biophysics
- <http://www.neuron.yale.edu/neuron/>
- L. O. Chua, L.Yang, 1988: “*Cellular Neural Networks: Theory*”. IEEE Trans. Circuits Syst., vol. 35.